

Dichroic effects in Auger photoelectron coincidence spectroscopy of solids

R. Gotter

Laboratorio Nazionale TASC-INFN, Area Science Park, S.S. 14 Km 163.5, I-34012 Trieste, Italy

F. Da Pieve, A. Ruocco, F. Offi, and G. Stefani

INFN, Unità Roma Tre and Dipartimento di Fisica, Università Roma Tre, Via della Vasca Navale 84, I-00146 Rome, Italy

R. A. Bartynski

Department of Physics and Astronomy and Laboratory for Surface Modification, Rutgers University, 136 Frelinghuysen Road, Piscataway, New Jersey 08854, USA

(Received 30 August 2005; revised manuscript received 18 October 2005; published 7 December 2005)

The Sn $M_5N_{45}N_{45}$ Auger spectrum from the $(\sqrt{3}\times\sqrt{3})R30^\circ$ -Sn/Ge(111) surface has been measured in coincidence with the corresponding $3d_{5/2}$ photoelectron. By detecting this pair at appropriate emission angles, the contribution from spin-symmetric (triplet) and spin-antisymmetric (singlet) final states can be selectively enhanced or suppressed. This dichroic effect in the Auger photoelectron coincidence spectroscopy of solids provides a probe of the local valence electronic structure with element, chemical states, emission depth, and spin selectivity. The consequences and applications of this dichroic effect are discussed.

DOI: [10.1103/PhysRevB.72.235409](https://doi.org/10.1103/PhysRevB.72.235409)

PACS number(s): 78.70.-g, 71.45.Gm, 79.60.-i

I. INTRODUCTION

Auger electron spectroscopy is a technique that is widely used to characterize the elemental composition of solid surfaces. Although it was realized early on that the line shape of Auger transitions contains considerable information about the local electronic structure of solids, such information can be difficult to extract owing to the complex decay processes involved. In recent years, however, advancements in core-hole excitation techniques and in the analysis of emitted electrons has sparked a renewed interest in Auger line shapes as an incisive probe of solids and their surfaces. For example, using synchrotron radiation as the excitation source, line shape studies of the Na $KL_{23}V$ Auger spectrum as a function of Na coverage on the Al(100) surface have demonstrated dramatic sensitivity of the Auger transition to the local surface environment.¹ Similarly, analyzing the energy distribution of emission electrons with Auger photoelectron coincidence spectroscopy² (APECS) provides an intrinsic state selectivity that arises from the coincidence detection of two electrons associated with a single-photoexcitation event. The study of the coincidence Pd $M_4N_{45}N_{45}$ Auger line shape of dilute Pd/Ag(100) surface alloys led to the discovery that the Coster-Kronig decay channel of the Pd $3d_{3/2}$ core hole is an order of magnitude larger in than in bulk Pd metal.³ Moreover, Auger electrons measured in coincidence with photoelectron loss features (and vice versa) give access to emission-depth selective line shapes for the study of thin layers on the nanometer scale.⁴ As advances in modern materials physics give rise to interesting new systems with ever more complicated chemical compositions, establishing a new selectivity in Auger transitions will make Auger spectroscopy an even more valuable technique for probing new materials.

In this paper we demonstrate that employing a moderate selection in angle to the APECS of solids can provide sensitivity to the spin coupling (i.e., triplet or singlet) in the Auger

final state, without the need to determine the spin of the emitted electrons. This additional discrimination extends the already known atomic specificity, chemical state, and emission-depth selectivity of the APECS technique.⁵⁻⁷ The observed behavior is an important generalization of results obtained from gas-phase targets.⁸ Extension to the solid state of these atomic physics findings is based on a previous angle-resolved (AR) APECS study of single-crystal Ge,⁹ which has demonstrated that solid-state effects, such as electron diffraction, do not obscure the essential properties of the atomic-source wave functions. In this study, the Sn $M_5N_{45}N_{45}$ Auger spectrum was measured in coincidence with Sn $3d_{5/2}$ core-level photoelectrons emitted from the $(\sqrt{3}\times\sqrt{3})R30^\circ$ -Sn/Ge(111) system. By placing rather loose constraints on the three vectors relevant to the kinematics of the experiment (i.e., the photon polarization vector $\vec{\epsilon}$ and the momentum vectors of the Auger and photoelectron \vec{k}_A and \vec{k}_p , respectively) spin-symmetric (triplet) and spin-antisymmetric (singlet) Auger final-state configurations are selectively enhanced or suppressed in the APECS spectra. This capability arises from the selectivity of AR-APECS on the magnetic quantum numbers m of the two-hole Auger final state¹⁰ and produces a spin-dependent asymmetry, i.e., a dichroic effect in angle-resolved Auger photoelectron coincidence spectroscopy (DEAR-APECS), which is here reported for the first time.

II. EXPERIMENT

Measurements were performed at the ALOISA beamline of the ELETTRA synchrotron facility in Trieste, Italy. A 1/3-atomic-layer-thick $(\sqrt{3}\times\sqrt{3})R30^\circ$ -Sn/Ge(111) surface was prepared in ultrahigh-vacuum conditions and monitored by observing the $(\sqrt{3}\times\sqrt{3})R30^\circ$ pattern along the $\langle 112 \rangle$ direction, in reflection high-energy electron diffraction. Details of the formation of this structure are given elsewhere.¹¹ The

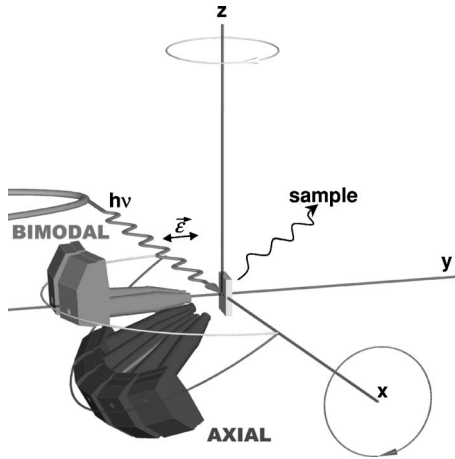


FIG. 1. Schematic representation of the analyzer frames in the ALOISA chamber.

chosen system is particularly well suited for our exploratory study because the proposed model is simple to apply (with a $4d$ closed shell and at submonolayer thickness) and the Sn $M_5N_{45}N_{45}$ Auger spectrum has strong and well-separated singlet and triplet contributions that are of roughly equal intensity.¹² In this way only aspects focused on the spin state will be relevant in discussing the Auger line shape.

The experimental setup, schematically depicted in Fig. 1, is discussed in detail elsewhere,¹³ and only a brief description is given here. Monochromatic, linearly polarized light impinging on the sample at grazing incidence, with the sample normal in the plane defined by \vec{e} and the propagation vector of the light \vec{k}_γ . The experimental chamber contains seven electron energy analyzers, each having an angular resolution of $\sim 1^\circ$, which can be positioned at different polar and azimuthal angles with respect to \vec{e} . Two of the analyzers sit on the so-called bimodal frame (plane xy in the figure), which can rotate around the z axis. The other five analyzers (termed axial) are positioned on a plane that contains the photon beam axis and that can rotate around the photon beam axis itself. Ten coincident pairs can thus simultaneously be acquired.

For the experiments presented here the coincidence kinetic energy distribution of Sn $M_5N_{45}N_{45}$ was measured under three geometric conditions. In one geometry (referred to as AA), both the photoelectrons and the Auger electrons were collected along directions aligned (A) (i.e., within $\sim 10^\circ$) with \vec{e} . In a second case (geometry AN), one electron of the pair was aligned with (i.e., collected along) \vec{e} while the other was not aligned (N) with \vec{e} but rather collected at polar angles of $\sim 55^\circ$. In a third case (geometry NN) both the photoelectrons and the Auger electrons were not aligned with \vec{e} . As an example the bimodal analyzers in Fig. 1 are, in our nomenclature, aligned with \vec{e} , while the axial analyzers are not aligned.

III. RESULTS AND DISCUSSION

Figure 2 shows the Sn $M_5N_{45}N_{45}$ Auger spectrum from the $(\sqrt{3} \times \sqrt{3})R30^\circ$ -Sn/Ge(111) surface, excited by 700-eV

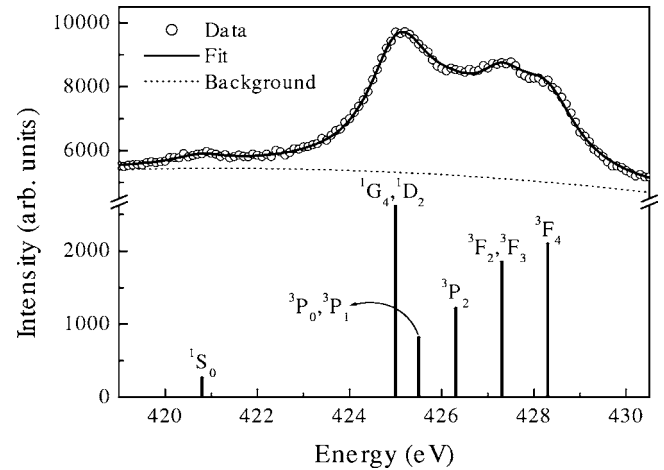


FIG. 2. Noncoincidence Sn $M_5N_{45}N_{45}$ Auger spectrum obtained from the $(\sqrt{3} \times \sqrt{3})R30^\circ$ -Sn/Ge(111) surface excited by 700-eV photons. The electron spectrometer energy resolution was 140 meV. The dotted line is a parabolic background, and the solid curve is a fit generated by the sum of Voigt profiles whose energy and relative intensity are given by the vertical bars indicating the multiplets of the d^8 final-state configuration (see Ref. 12).

photons. The bars identify relative energies and intensities of the d^8 two-hole Auger final-state multiplets. The spectrum is dominated by two contributions. From the multiplet assignment by Parry-Jones *et al.*,¹² the peak at lower kinetic energies is associated primarily with the 1G and 1D states while the peak at higher kinetic energies originates from the 3F multiplet. In addition, there is a relatively weak feature assigned to the 1S component.

Figures 3(a) and 3(b), top panels, compare the APECS Auger line shapes (symbols with error bars) taken in geometries AN_1 , NN , and AN_2 , AA , respectively [AN_1 and AN_2 are two realizations of the AN geometry: the first case is photoelectron-(A -) Auger (N) while the second case is a mixed configuration, which includes also some photoelectron- (N -) Auger (A) pairs]. It is clear from Fig. 3 that the coincidence spectra differ from the singles spectra, as measured at the same time and by the same analyzers, and that they do so in very different ways. In particular, the coincidence spectra taken in geometries AA and NN (black solid squares) have a lower relative intensity in the region of the 3F triplet while the coincidence spectra taken in AN geometries (open circles) have a reduced intensity in the region associated with the 1G and 1D singlets. In the region associated with the 1S term, no sizable difference among the several spectra is seen. In order to exclude possible artifacts due to sample conditions or instrumental alignment, the coincidence spectra reported in Fig. 3(a), top panel—i.e., AN_1 and NN —were acquired simultaneously with the same Auger analyzer, in coincidence with photoelectrons of the same energy. The spectra differ only with respect to the emission angle of the coincident photoelectron.

The behavior of the coincidence spectra can be understood by considering the relevant selection rules.¹⁴ The photoelectron and Auger electron wave functions have predominantly f and d character, respectively; hence, neglecting scattering effects, the angular distributions are essentially de-

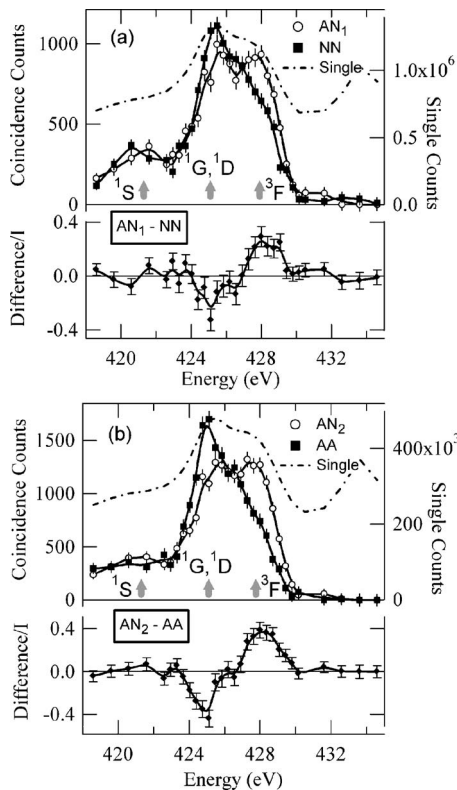


FIG. 3. Auger spectra obtained in coincidence with Sn $3d_{5/2}$ photoelectrons are shown in (a) and (b) top panels. The data points with error bars are the coincidence data (the superimposed solid line is a guide to the eyes), and the dashed line is the simultaneously acquired single spectrum. The Auger channel energy resolution was 1.4 eV while it was 3 eV for the photoelectron channel. The geometries of the measurements were designed to suppresses the contribution from symmetric-spin states (AN_1 and AN_2) or antisymmetric-spin states (NN and AA). The bottom panels of (a) and (b) show the dichroic effect in angle-resolved Auger photoelectron coincidence spectroscopy (DEAR-APECS) as derived from the difference between the spectra reported in the corresponding top panels.

terminated by the associated spherical harmonics. As the photons are linearly polarized along $\vec{\epsilon}$, the photoelectron selection rules dictate that the magnetic quantum number of the core hole, m_C , is equal to that of the photoelectron. From Auger selection rules and under the hypothesis that the expansion of the Coulomb interaction can be limited to the first order—i.e., when the κ parameter is equal to zero (see Ref. 14)—it can be derived that $m_1 = m_C$ and $m_2 = m_A$ (where m_A , m_1 , and m_2 are the magnetic quantum numbers of the Auger electron and the two final state holes, respectively), and hence $\Delta m = (m_1 - m_2) = (m_C - m_A)$. Previous studies of Auger and photoelectron diffraction patterns^{15,16} have established that collecting electrons ejected close to $\vec{\epsilon}$ favors $m=0$ components of the emitted electrons' partial waves, while larger m components are predominant at larger ejection angles [$|m| \geq 1$ for electrons emitted at angles bigger than 55° (Ref. 10)]. This means that the dominant contributions are, for the AA geometry, $m_C = m_A = 0$, so $|\Delta m| = 0$; for the AN geometry, $m_C = 0$ and $|m_A| \geq 1$ (and vice versa), so $|\Delta m| \geq 1$; while for the geometry NN , $|m_C|$ and $|m_A| \geq 1$, which means $|\Delta m| \leq 1$

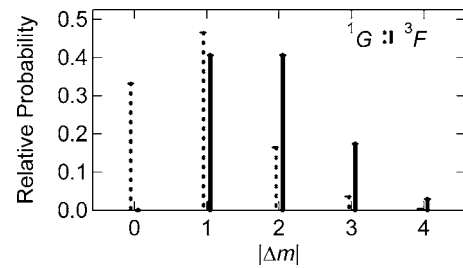


FIG. 4. Predicted contributions to the 1G and 3F multiplets as a function of the difference in magnetic quantum numbers, $|\Delta m| = |m_1 - m_2|$, of the two holes in the Auger final state. Note that the 3F state has no weight with $|\Delta m| = 0$ but dominates for $|\Delta m| \geq 2$.

or ≥ 3 (with the first as the dominant one: see Fig. 4 and related discussion).

To understand the different behavior of the coincidence spectra it is helpful to recall that the multiplet of the Auger final state can be written, in a simple closed-shell model, as linear combinations of one-electron product states with different m 's:

$$|L, M\rangle = \sum C_{l_1 m_1 l_2 m_2}^{LM} |l_1 m_1\rangle |l_2 m_2\rangle, \quad (1)$$

where L and M are the total angular momentum and its z projection, respectively, for the two-hole states and the $C_{l_1 m_1 l_2 m_2}^{LM}$ are the Clebsch-Gordan coefficients (l_1 and l_2 are the orbital quantum numbers of the two-hole final states). Figure 4 shows their relative weight that contributes to the 1G and 3F multiplets, arranged according to the difference $|\Delta m|$. As is typical, the wave functions of triplet states are weighted toward large $|\Delta m|$ while singlets favor smaller $|\Delta m|$.¹⁰ In the AA geometry, $m_1 = m_2$, so only final states where both holes have all spatial quantum numbers identical will contribute. Therefore, only states with antisymmetric spin wave functions (i.e., singlets) participate in the APECS signal. Also the NN geometry ($|\Delta m| \leq 1$ or ≥ 3) has the 1G as the dominant configuration (see Fig. 4) and, therefore, even though the kinematics of the experiment are quite different, the coincidence Auger line shape should be similar to that measured in AA geometry. This is borne out in the top panels of Figs. 3(a) and 3(b) where the 3F multiplets are suppressed in both NN and AA spectra. In AN geometries, final states with $|\Delta m| \geq 1$ dominate, so the 1G contribution should be significantly suppressed with respect to that of the 3F , just as is observed in the AN_1 and AN_2 spectra.

The selectivity of these spectra can be characterized by the DEAR-APECS asymmetry spectrum which we define as

$$\text{DEAR-APECS}(E) = \frac{AN(E) - AA(E)}{\frac{1}{2} \sum_i [AN(E_i) + AA(E_i)]}. \quad (2)$$

The DEAR-APECS for the Sn $M_5N_{45}N_{45}$ transition is shown in the bottom panel of Fig. 3(b), while the corresponding asymmetry spectrum for the AN - NN geometries is shown in

the bottom panel of Fig. 3(a). From Eq. (2), the singlet components have a negative asymmetry while the triplet components have a positive one. A vanishing asymmetry is apparent from the figure for the 1S multiplet, as it must because in its wave function each possible even value of $|\Delta m|$ is equally represented and all odd values of $|\Delta m|$ are absent.

We note that, in the core-core-core Sn $M_5N_{45}N_{45}$ Auger decay, all levels involved are closed shells in the initial state and therefore have no intrinsic preferred orientation, as would be the case for an open shell with finite magnetic moment. Nevertheless, the APECS measurements are selective to the spin coupling in the final state. In the present case, the asymmetry arises from the multiplet nature of the Auger final state and can therefore be very helpful in resolving the multiplet contributions to the Auger spectra of complex materials. However, it is also true that by properly choosing the experimental geometry the DEAR-APECS amplitude can be tuned so that this geometry-induced asymmetry is zero. Under such conditions, any intrinsic asymmetry that may lead to unequal populations of the m levels in a system, such as structural or magnetic anisotropies, can be revealed. In magnetic systems this is particularly interesting as it may enable one to probe the local valence-level spin configuration of a particular ion in a particular state in the sample. As the APECS process is referenced to the local spin, DEAR-APECS is expected to be nonzero for materials with ferromagnetic or antiferromagnetic ordering, or even for a system with a local moment, such as a disordered paramagnet. For example, in the case of an itinerant ferromagnet, such as iron at temperatures below the Curie temperature, unequal populations of majority- and minority-spin states will produce a nonzero DEAR-APECS whose energy distribution is determined by the local spin density of states. The observation of DEAR-APECS from a magnetic system would provide a

new method to probe spin-dependent properties of the valence levels, which joins a number of already well-established spectroscopies based on dichroic effects.¹⁷ It complements information on occupied electronic states that can be probed with spin selectivity by magnetic circular dichroism in x-ray emission,¹⁸ with the added value that it is particularly well suited for investigating low-dimensional systems on the nanometer scale where local environment¹ and emission-depth⁴ selectivity are of paramount importance.

In recent years, the application of APECS to study solids has been increasing^{2,10,19} and most such experiments provide some degree of angular selection and light helicity (as with synchrotron radiation). The discovery of the DEAR-APECS effect, i.e., an experimentally imposed nonstatistical weight of the multiplet component intensity, suggests to critically reconsider the above mentioned APECS experiments as this effect may be relevant to their interpretation.

In conclusion, we have measured the Sn $M_5N_{45}N_{45}$ Auger spectrum in coincidence with Sn $3d_{5/2}$ photoelectrons excited with linearly polarized light and emitted in specific directions with respect to $\vec{\epsilon}$. In the appropriate geometry, the contributions from final states with symmetric- or antisymmetric-spin wave-functions to the coincidence Auger spectrum can be enhanced or suppressed. This spin selectivity provides the opportunity for new applications in the field of nanosized materials.

ACKNOWLEDGMENTS

The authors are grateful to the ALOISA beamline staff members for the valuable support provided during the experiments at ELETTRA, and they are also indebted to INFN for financial support provided through the ‘‘Supporto ELETTRA’’ program. One of us (R.A.B.) acknowledges support by the NSF under Grant No. ECS-0224166.

-
- ¹M. I. Trioni, S. Caravati, G. P. Brivio, L. Floreano, F. Bruno, and A. Morgante *Phys. Rev. Lett.* **93**, 206802 (2004).
- ²R. A. Bartynski, E. Jensen, S. L. Hulbert, and C.-C. Kao, *Prog. Surf. Sci.* **53**, 155 (1996).
- ³D. A. Arena, R. A. Bartynski, R. A. Nayak, A. H. Weiss, S. L. Hulbert, and M. Weinert *Phys. Rev. Lett.* **91**, 176403 (2003).
- ⁴W. S. M. Werner, W. Smekal, H. Störi, H. Winter, G. Stefani, A. Ruocco, F. Offi, R. Gotter, A. Morgante, and F. Tommasini, *Phys. Rev. Lett.* **94**, 038302 (2005).
- ⁵H. W. Haak, G. A. Sawatzky, and T. D. Thomas, *Phys. Rev. Lett.* **41**, 1825 (1978).
- ⁶E. Jensen, R. A. Bartynski, S. L. Hulbert, E. D. Johnson, and R. Garrett, *Phys. Rev. Lett.* **62**, 71 (1989).
- ⁷P. Le Fèvre, J. Danger, H. Magnan, D. Chandresris, J. Jupille, S. Bourgeois, M.-A. Arrio, R. Gotter, A. Verdini, and A. Morgante, *Phys. Rev. B* **69**, 155421 (2004).
- ⁸N. M. Kabachnik, *J. Phys. B* **25**, L389 (1992).
- ⁹R. Gotter, A. Ruocco, M. T. Butterfield, S. Iacobucci, G. Stefani, and R. A. Bartynski, *Phys. Rev. B* **67**, 033303 (2003).
- ¹⁰G. Stefani, R. Gotter, A. Ruocco, F. Offi, F. Da Pieve, S. Iacobucci, A. Morgante, A. Verdini, A. Liscio, H. Yao, and R. A. Bartynski, *J. Electron Spectrosc. Relat. Phenom.* **141**, 149 (2004); G. Stefani, R. Gotter, A. Ruocco, F. Offi, F. Da Pieve, A. Verdini, A. Liscio, S. Iacobucci, H. Yao, and R. A. Bartynski, in *Correlation Spectroscopy of Surfaces, Thin Films, and Nanostructures*, edited by J. Berakdar and J. Kirschner (Wiley-VCH, Weinheim, 2004), p. 222.
- ¹¹L. Floreano, L. Petaccia, M. Benes, D. Cvetko, A. Goldoni, R. Gotter, L. Grill, A. Morgante, A. Verdini, and S. Modesti, *Surf. Rev. Lett.* **6**, 1091 (1999); L. Petaccia, L. Floreano, M. Benes, D. Cvetko, A. Goldoni, L. Grill, A. Morgante, A. Verdini, and S. Modesti, *Phys. Rev. B* **63**, 115406 (2001).
- ¹²A. C. Parry-Jones, P. Weightman, and P. T. Andrews, *J. Phys. C* **12**, 1587 (1979).
- ¹³R. Gotter, A. Ruocco, A. Morgante, D. Cvetko, L. Floreano, F. Tommasini, and G. Stefani, *Nucl. Instrum. Methods Phys. Res. A* **467-468**, 1468 (2001).
- ¹⁴P. J. Feibelman, E. J. McGuire, and K. C. Pandey, *Phys. Rev. B* **15**, 2202 (1977).
- ¹⁵D. E. Ramaker, H. Yang, and Y. U. Idzerda, *J. Electron Spectrosc. Relat. Phenom.* **68**, 63 (1994).

¹⁶Y. U. Idzerda, Surf. Rev. Lett. **4**, 161 (1997).

¹⁷See, for example, H. Ebert, Rep. Prog. Phys. **59**, 1665 (1996); W. Kuch and C. M. Schneider, *ibid.* **64**, 147 (2001); H. Wende, *ibid.* **67**, 2105 (2004), and references therein.

¹⁸F. M. F. de Groot, M. Nakazawa, A. Kotani, M. H. Krisch, and F.

Sette, Phys. Rev. B **56**, 7285 (1997); S. Eisebitt, J. Luning, J. E. Rubensson, D. Schmitz, S. Blügel, and W. Eberhardt, Solid State Commun. **104**, 173 (1997).

¹⁹S. M. Thurgate, J. Electron Spectrosc. Relat. Phenom. **100**, 161 (1999).